A Deep Learning-Based Modeling of a 270 V-to-28 V DC-DC Converter Used in More Electric Aircrafts

Gabriel Rojas-Dueñas, Jordi-Roger Riba, *Member, IEEE*, and Manuel Moreno-Eguilaz

***Abstract*—This article presents a novel approach for black-box modeling of 270 V-to-28 V dc–dc step-down converters used in more electric aircrafts. These converters normally feed constant power loads. The proposed deep learning approach, uses offline experimental data of the converter to find an accurate model that reproduces its behavior. It covers a broad range of loading conditions to build a model that replicates the whole behavior of the converter. This article compares the performance of the proposed method, which requires a very low computational burden once the model is trained, with that of a conventional recurrent neural network topology. Results presented in this article show the ability of the obtained solution to accurately emulate the behavior of the real step-down converter when the internal structure is unknown, with no knowledge of the internal parameters, thus preventing disclosure of manufacturer's confidential data. The modeling strategy presented in this article is validated with experimental data by using a step-down converter used in aircrafts. The approach is compared to existing modeling techniques to test its accuracy. This approach can also be applied to many power devices, including diverse types of power converters, power supplies, or filters among others.**

***Index Terms*—Black-box models, dc–dc power converters, deep learning, modeling, neural networks, simulation, transient response.**

I. Introduction

SWITCHED mode dc–dc converters are applied in several areas, including power systems, renewable energy systems [1], automotive [2] or aerospace [3] among others, since they have appealing features, including high efficiency, power density and reliability [4]. For the particular case of the more electric aircraft (MEA), there are numerous power converters, inverters and filters, which tend to improve their processes and efficiency in order to satisfy the new necessities. Power converters exhibit an inherent nonlinear behavior due to the switching action of the power switches, thus making its modeling difficult due to the complexity of the required models [5]. MEA power systems designers require efficient and accurate modeling tools, which must be able to reproduce even the small details of the steady state and transient responses to validate the behavior of the prototypes in the course of the power system design and optimization stages. Conventional modeling relies on thorough knowledge of the values of the dc–dc converter parameters, both the passive elements and the control circuit. In addition, complex power systems include power converters delivered by different manufacturers [3]. Modeling of power converters in such conditions is not an easy task, since converters from different manufacturers, the characteristics of the source or the load type have a deep impact on the dynamics [6]. Even so, some details of the response depend on parasitic elements, which are often difficult to model when using classical simulation models, especially when analyzing high-frequency switched converters. However, the manufacturers of dc–dc converters often provide partial or limited information about the internal components [7], and thus, the data available in the datasheets usually is not enough to generate accurate simulation models with a high level of detail [8]. For example, power systems in large passenger aircrafts usually combine several models of dc–dc converters from different manufacturers, thus making it difficult to generate accurate dynamic models [9]. In addition, accurate models should be able to reproduce ripples in the currents and voltages, transients due the turn-on and turn-off operation in the switches, the effects of external disturbances, variable ambient conditions or component degradation among others, which can have a nonnegligible impact on the behavior of the dc–dc converter [9].

Different approaches are available to model dc–dc converters. They can be roughly classified into white-, black- and grey-box models. White-box models require a deep physical description of the converter through a set of algebraic or differential equations, which are able to reproduce its dynamics [10]. On the other hand, gray-box models consist of a data-driven approach where the prior knowledge about the system is available, but is limited. Contrarily, black-box models, such as the ones applied in this article, do not assume any particular structure of the converter, so that they are able to emulate or reproduce its behavior without describing its physical equations [9] when the internal topology is unknown, so that this model does not require internal data of the converter. Therefore, black-box models prevent disclosure of manufacturer's confidential data [3], [5]. In addition, once the model is trained, it requires low computational burden. Black-boxes have been applied to model different types of devices, such

Manuscript received March 31, 2021; revised June 7, 2021; accepted July 15, 2021. Date of publication July 21, 2021; date of current version September 16, 2021. This work was supported in part by the Generalitat de Catalunya under Project 2017SGR0967 and in part by the European Commission through the Clean Sky Program, under Project 755332-AEMSIdFit. Recommended for publication by Associate Editor S. C. Tan. *(Corresponding author: Jordi-Roger Riba.)*

Gabriel Rojas-Dueñas and Jordi-Roger Riba are with the Department of Electrical Engineering, Universitat Politècnica de Catalunya, Terrassa 08222, Spain (e-mail: gabriel.esteban.rojas@upc.edu; riba@ee.upc.edu).

Manuel Moreno-Eguilaz is with the Department of Electronics Engineering, Universitat Politècnica de Catalunya, Terrassa 08222, Spain (e-mail: manuel.moreno.eguilaz@upc.edu).

Color versions of one or more figures in this article are available at https://doi.org/10.1109/TPEL.2021.3098468.

Digital Object Identifier 10.1109/TPEL.2021.3098468

as dc–dc converters [11], battery chargers [12], or permanent magnet generators [13], among others.

Several black-box approaches to model power converters are found in the technical literature, most of them being based on transfer functions, which are parametrized in the frequency domain. However, this approach presents several drawbacks, because of the errors due to the conversion from frequency to time domains or vice versa, or the need to use expensive measuring devices and complex tests, particularly when analyzing high power converters [3]. In [6] and [11], it is presented a black-box approach based on a two-port equivalent circuit, which is parametrized in the frequency domain. The four parameters of the two-port matrix are transfer functions, which are obtained by using a high-frequency impedance analyzer. However, these works assume that the average value of the output voltage is known, which is used to build the model, only the continuous conduction mode is analyzed and the presented results are based only on two/three load conditions. A similar approach is applied in [14] and [15], where the black-box model of a three-phase ac–dc converter is obtained from frequency-domain response data. An electromagnetic compatibility black-box model of a dc–dc converter operating in open-loop configuration based on wavelet transform and support vector regression is presented in [5]. The Hammerstein model is presented in [16], it models the nonlinear and the linear dynamic characteristics separately and generates an overall transfer function based on this two models. It results on a simple and accurate model; however, it is subjected to the operating point of the dc–dc converter. A black-box model based on time-domain measurements is presented in [3], which identifies the transfer function coefficients from input voltage and current steps. However, such approach requires to select a predetermined candidate transfer function and the posterior application of a suitable optimization algorithm [8]. Considering the modeling of MEA converters, in [3] a dc–dc converter of a fuel cell unit of an aircraft is modeled using a polytopic model that is based on local transfer functions of the converter [17]. This method is based on an input current control, which implies that different current steps are needed, adding complexity to the experimental setup. In [18] and [19], a modeling technique based on the state-space average equations of the converter is explained, it uses a known topology of the converter to generate a transfer function that is tuned with measured data.

This article proposes a deep learning methodology to obtain an accurate and replicable offline data-driven model of a 270 V-to-28 V dc–dc converter used on the on-board system of MEA. It uses long short-term memory neural networks (LSTM-NNs) to generate the model and its hyper-parameters are tuned by means of a Bayesian optimization algorithm (BOA). In [20], a converter modeling method based on LSTM-NN is proposed. However, it uses simulated data, the hyperparameters are not optimized, the ripple of the signals is not estimated and the immediate transient response is not replicated with accuracy. The approach proposed in this article is different from the solutions found in the technical literature and contributes to the state-of-the art in several aspects. First, it allows reproducing the steady state and transient behaviors of the power converter by acquiring the input-output voltages and currents, that is, by means of time-domain measurements. This is advantageous since it simplifies the requirements of the measuring equipment and avoids transformations from the frequency to the time domain and vice versa, which is required in many other approaches [6], [11]. Second, the measurements are non-invasive and independent of the converter topology, it does not require to continuously apply an excitation signal to the converter, which is the case of the Hammerstein model [16]. Third, this modeling approach is very robust and accurate, since it is able to reproduce the dynamics of the dc–dc converter under different operating points and under the continuous and discontinuous conduction modes (CCM and DCM). Other approaches [6], [16], [17] require different models depending on the operating point, and some others are unable to integrate the CCM and DCM in just one model. Fourth, the approach proposed here is based on a real case, since the behavior of a high voltage 270 to 28 V dc–dc converter used in aircrafts is identified with high accuracy by having connected realistic constant power loads (CPLs), while most of previous works have simple setups and converters where the industrial application is not clear [6], [18], [19]. Fifth, it outperforms other deep neural network models because it does not consider a fixed length of the data, and the computational burden is lower [21]. Finally, the obtained model can be easily integrated in an electrical simulation environment because it consists of just one model that generates an output based on matrix operations. The proposed methodology can be adapted to a wide range of devices, including diverse types of power converters, power supplies, or filters among others. The modeling approach is compared to two other neural network architectures and two techniques are compared to the one based on nonlinear autoregressive exogenous neural network (NARX-NN) presented in [22].

II. Proposed Black-Box Model of the DC–DC Converter

A black-box model allows reproducing the behavior of a device with unknown structure and unknown internal parameters, which is often characterized by means of the input and output signals [3]. This section proposes an offline system identification methodology that main objective is to obtain a model of a 270 V-to-28 V dc–dc converter when there is no prior information about its topology or electrical characteristics. It is based on the well-known deep learning algorithm named LSTM-NN. Also, to enhance the accuracy of the model, a set of hyperparameters of the NN is defined by applying an optimization algorithm.

Fig. 1 describes the proposed methodology for obtaining a NN that describes the behavior of the converter. It shows that the tuning of the hyperparameters of the NN is a key stage. The learning rate (LR), which refers to how fast the weights of the NN are adjusted, is tuned by means of the LR range test. The next step is to apply the BOA to determine the value of each hyperparameter using the pre-processed training and validation datasets. If the lowest value of the root-mean-square error (RMSE) is below than the defined threshold, the combination of hyperparameters is stored, otherwise, the set of hyperparameters are redefined and the process starts again. After having a proper

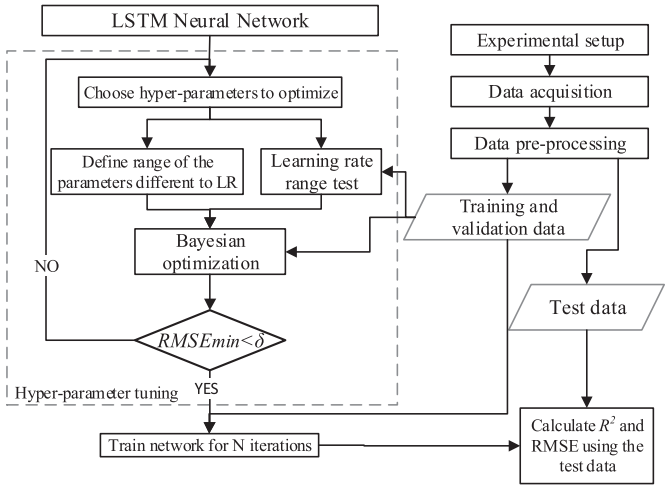

Fig. 1. Proposed algorithm to train LSTM neural networks.

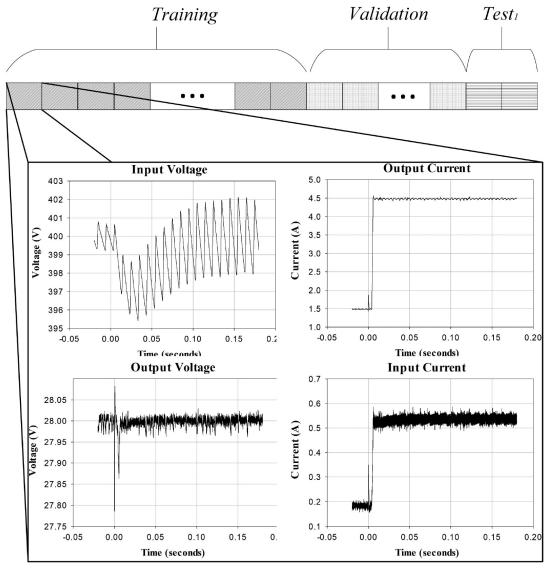

Fig. 2. Distribution of experiments.

configuration of hyperparameters, the network is trained again for N iterations and then, the determination coefficient R^2 and the RMSE are calculated using the preprocessed test dataset to measure the accuracy of the model. It is important to mention that for the LR range test and the BOA, just a fraction of the total number of iterations (N) are considered in order to accelerate the process.

The following subsections present an explanation of the working principle of the LSTM-NN and how the hyperparameters of it are tuned based on the data acquired from the dc–dc converter.

A. Problem Definition

First of all, it is necessary to define the main characteristics of a dc–dc converter in order to explain how the LSTM-NN is used to generate a model of it. Considering that there is no prior knowledge about the internal structure of the converter, the only accessible information is the measurements at the input and output terminals, which for this article are the voltages and currents. Since the proposed methodology aims to model the static (ripple) and dynamic characteristics of the converter, the sampling frequency needs to be higher that the commutation frequency of the converter. A deeper explanation regarding the 270 to 28 V dc–dc converter and its data acquisition system is given in Section III.

The inputs of the black-box (LSTM-NN) are the input voltage and output current, because these are the variables that can be controlled externally by means of changing the voltage input level or the output load, respectively, whereas the outputs are the input current and output voltage. Consequently, the modeling of the power converter is considered a regression problem, since it aims to generate two numeric and dependent output variables as a function of the inputs. The length of the data is determined by the number of points recorded in the measurements. The LSTM-NN depth and its hyperparameters are adjusted based on the dataset characteristics, as it is described in the following subsections. The data used to train the NN is organized in three different groups, i.e., training, validation and test datasets. The first two are used for the training process and the last one to test the accuracy. Each dataset has a certain number of experiments, each experiment consisting of a load change. Fig. 2 shows the experiments corresponding to the different datasets.

After the LSTM-NN is trained, the RMSE and the R^2 are calculated for different operating conditions of the converter and its mean value is calculated. A value of the R^2 equal or almost 1, since it indicates a strong correlation between the measurements and the model output.

B. Long Short-Term Memory Neural Network

LSTM-NNs were first introduced in 1997 [23] as a necessity to overcome the long-term dependency problem, which is associated to the gradient decay that occurs in traditional RNNs. LSTM-NNs preserve the backpropagation error over time and across the layers of the NN, which is useful because it allows the network to discard the irrelevant information for the training stage, and the weights are updated according to memory units protected from perturbations. This topology allows the NN to keep learning even if there are many time steps, as it is the case of this article.

The LSTM cell consists of memory blocks that are able to store, write, read or forget information by means of gates that open and close, depending on the correspondent weights [24]. Fig. 3 shows the complexity of the LSTM cell when compared with a normal one. In Fig. 3, h refers to the cell value, c represents the cell memory state, x the input value and σ the sigmoid function. In order to understand Fig. 3, it is important to mention that there is a module (or cell) for each step of the time series. In general, it is a chain where the future output depends on past inputs and outputs.

Fig. 3 shows that in a standard RNN, the cell only uses one gate, which is an activation function (usually tanh). The LSTM cell has three gates: input (I); output (O); and forget (F), that interact with each other and control the cell state. In addition, inside the cell there are pointwise operations that occur at the

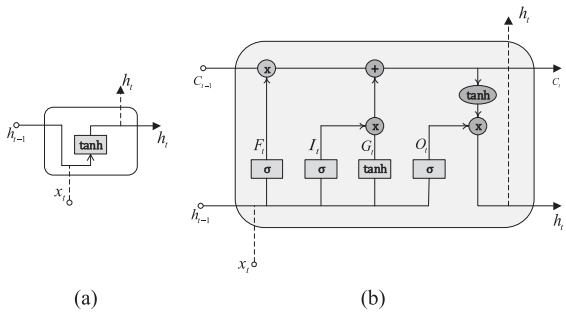

Fig. 3. Cell structure. (a) Traditional RNN. (b) Long short-term memory.

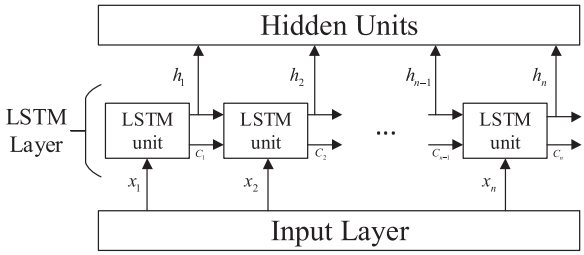

Fig. 4. LSTM blocks connections.

gates, and are presented in (1)–(3), whereas (4) describes the calculation of the cell input activation vector

$$I_t = \sigma\left(W_i x_t + R_i h_{t-1} + b_i\right) \tag{1}$$

$$F_t = \sigma\left(W_f x_t + R_f h_{t-1} + b_f\right) \tag{2}$$

$$O_t = \sigma\left(W_o x_t + R_o h_{t-1} + b_o\right) \tag{3}$$

$$G_t = \tanh\left(W_g x_t + R_g h_{t-1} + b_g\right) \tag{4}$$

where W is the weights of the respective gate, R is the recurrent weights, and b is the bias values. The sigmoid function in (1)–(3) generates values between 0 and 1, depending on the relevance of the input data [24]. The next step is to calculate the memory and hidden states of the cell, as shown in

$$c_t = F_t \cdot c_{t-1} + I_t \cdot G_t \tag{5}$$

$$h_t = O_t \cdot \tanh\left(c_t\right). \tag{6}$$

Finally, the output values of the cell unit are calculated as a function of the hidden states as

$$y_t = W_{fc} h_t + b_{fc} \tag{7}$$

where W_{fc} and b_{fc} are the weights and bias of the fully-connected layer, respectively.

The structure of the LSTM allows the network to learn the long range temporal dependencies from the dataset used to train [25]. This characteristic is especially useful for the system identification of dc–dc power converters, because the previous time steps affect the outputs of the black-box system. All processes described in Fig. 3 are just for one cell or block. Fig. 4 shows the general perspective of the hidden layer of the network, where the input layer refers to the inputs of the system and hidden units are the neurons.

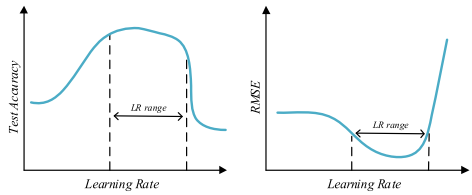

Fig. 5. Loss and accuracy versus LR.

The number of LSTM cells in Fig. 4 corresponds to the number of time steps of the dataset. The input x_j of the black-box system is sent to the LSTM cell, the x_j vector consisting of the input values of the system at the time step *j*. The h_j term is the output of the LSTM cell and contains the weights of the neurons at the *jth* time step, while c_j represents the updated cell state.

The overall structure of the NN consists of four layers, the sequence input layer, hidden layer (LSTM), Fully connected layer and the regression output layer.

C. Hyperparameter Tuning

According to the proposed algorithm in Fig. 1, the first step is to select the hyper-parameters to be tuned, which depend on the solver. In this article, the "Adam" solver was used, because it shows good performance for deep NNs dealing with time series [26]. This type of solver consists on several hyper-parameters, and each one affects in a different way the training of the NN. In order to limit the configuration space of the hyper-parameters in the optimization process, just five of them were chosen. These are the LR, neurons of the LSTM layer, decay rate and the L2 regularization. These are the hyper-parameters with most influence over the convergence, accuracy, computational burden and pattern identification [27].

The LR is one of the most important hyper-parameters to tune in a neural network. If the LR is too small, it requires more training time, and can produce overfitting. If the LR is too large, the training may diverge. Therefore, the LR range test [28] is used to find a correct value or range of values of the LR in order to improve accuracy and decrease the training cost. The test is simple and consists of training a set of NNs while the LR increases in each iteration. The LR is initially set to a small value, so that it increases linearly until the training diverges. The values of the loss function, RMSE and accuracy are stored at each iteration, as shown in Fig. 5.

To select the appropriate bounds or the LR, the following assumptions are considered [28]. The minimum LR bound corresponds to a tenth of the maximum bound, whereas the maximum bound is chosen according to the divergence of the training. For this article, the training of each network will only consider the first 50 epochs. The LR range is used as an input for the Bayesian optimization, as explained in the next section.

1) Bayesian Optimization Algorithm: It must be noted that traditional methods such as grid search and random search require a significant number of iterations to find a proper configuration of the NN during the training stage. For large datasets or complex structures, each iteration may take a long time, so the cost of evaluating the objective function using the

aforementioned methods can be too high. As explained, the BOA is well-suited for this purpose, since it finds an optimal set of hyper-parameters after training a small number of networks. This method uses a probabilistic surrogate model of an unknown objective function $f(x)$, so that the optimization problem is as follows [29]:

$$x^* = \arg\max_{x \in X} f(x) \tag{8}$$

where X is the space of possible values of the hyper-parameters to be tuned and x^* is the optimal solution. The function of the model can be considered as a stochastic Gaussian process because it combines the distribution of each hyperparameter.

The BOA is a sequential method, since it considers the past evaluation results to select a new set of parameters that may outperform the last ones in the surrogate function. The main objective is to update $f(x)$ at each iteration to reduce the uncertainty of the model and to obtain a more accurate result. The last iteration is not necessarily the best one, but it helps to build the probabilistic model and to be closer to a more accurate solution [29]. The key elements of BOA are the model of the function and the acquisition function. The first refers to the surrogate function, which for the case of LSTM-NN's hyperparameters, it is a Gaussian process, as mentioned before. The second one refers to the function to be optimized to find the location of the next observation, by evaluating the candidate points in the surrogate function. The chosen acquisition function was the expected improvement per second plus [30]. Choosing the correct functions gives a good balance between exploration (large uncertainty in the surrogate model) and exploitation (model prediction is high), which is desirable.

III. 270 V-TO-28 V STEP-DOWN DC–DC CONVERTER

This section describes the part on the right of Fig. 1, which is related to the acquisition of the data that is used to generate the model of the dc–dc converter. It presents a general overview of the on-board system of the MEA and the implementation of it in the laboratory.

A. MEA On-Board Distribution System

DC distribution systems of the MEAs consist of several motors, power electronics devices, batteries, CPLs and others [31]. Normally, the high voltage (HV) dc bus operates at 270 V, whereas the low voltage dc bus operates at 28 V [32]. Therefore, the dc–dc converter to be identified in this article is a step-down converter where the input voltage is 270 V and the output level is 28 V. The loads are modeled as CPL, which result of connecting a resistive load to a dc–dc power converter.

Fig. 6 shows the schematic of a typical on-board distribution system of an aircraft. It can be seen that the signal generated by the synchronous generator (G) is rectified to a dc signal with a voltage level of 270 V. The 270 V bus feeds different loads, where one of them is the isolated and regulated dc–dc converter. This converter represents the black-box to be identified by using the training algorithms explained in the previous sections. Several CPLs (dc–dc power converter with a resistive load) are connected to the 28 V bus at the output of the aforementioned converter.

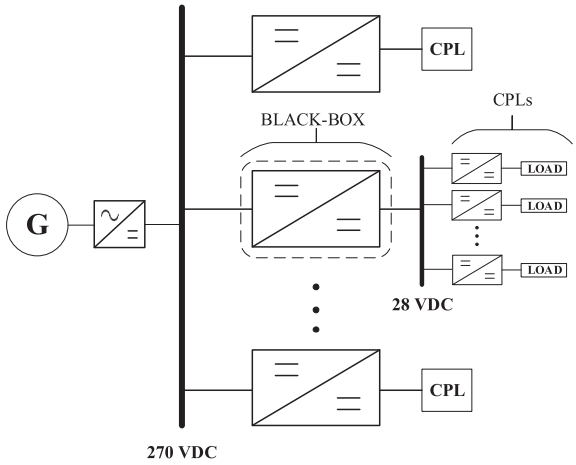

Fig. 6. MEA on-board distribution system.

Considering the nature of the 270 HVdc, where the voltage delivered is always 270 V with minor perturbations [32], the input voltage of the step-down converter (black-box) is set as constant for all the experiments and the level might change in a range of 240 to 300 V. Then, to obtain a complete dataset to train the neural networks, it is necessary to acquire data of the step-down converter under different load conditions. In addition, each experiment includes a load change (perturbation) to represent accurately the transient behavior of the power converter. However, the transient generated due to a sudden change of the input voltage is not considered, because the transition between two output values of the voltage source used for this purpose takes more time that that required for the control loop controller. The chosen CPLs should cover a wide output power range of the step-down converter, from low values up to the rated power.

It is important to mention that in many cases the manufacturer of the power converter does not provide any information regarding the corresponding conduction modes. Therefore, from a black-box point of view (input and output measurements) it is not possible to distinguish whether the converter is in CCM or in DCM. To overcome this problem, a wide range of operation of the converter was considered.

B. Experimental Setup

This section presents the procedure carried out to acquire the data required for an accurate modeling and training of the NNs. As explained, a rich dataset is needed, which means a considerable number of scenarios and load changes in order to fully represent the steady state and the transient response of the dc–dc converter. Considering that the output load may change at every experiment, and a large number of experiments is needed, the acquisition of the experimental data was automated and controlled externally using a computer, as shown in Fig. 7. The output load consists of eight CPLs (dc–dc converter with a resistor) connected in parallel. Each CPL is connected in series with a power transistor. By this way the CPLs can be

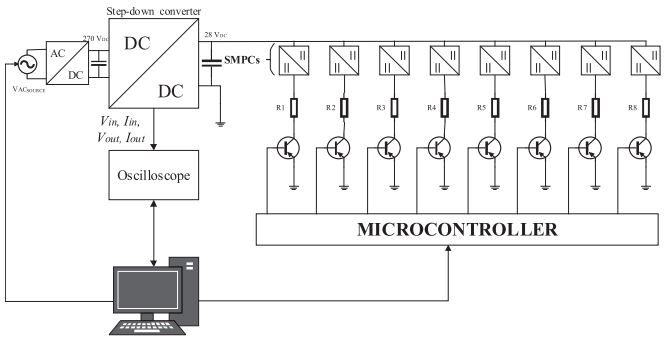

Fig. 7. Experimental setup to acquire the datasets.

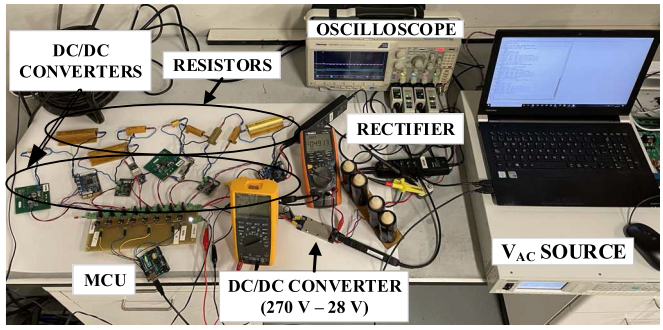

Fig. 8. Experimental setup in the laboratory.

TABLE I
VICOR DCM3714xD2K31E0YZZ STEP-DOWN CONVERTER SPECIFICATIONS

Parameter	Value
Input voltage range	160 V – 420 V
Output voltage	28 V
Maximum output power	500 W
DCM load condition	< 50 W
Switching frequency	700 kHz
Peak efficiency	93.7 %

TABLE II
DC–DC CONVERTERS SPECIFICATIONS

Type	Units	Manufacturer	Reference	V_{out}(V)	P_{max} (W)	f (kHz)
Buck	2	Texas Instruments	TPS40200EVM-002	3.3	8.25	200
Buck-Boost	2	Vicor	PI3741-01-EVAL1	48	150	750
Forward	2	Maxim Integrated	MAX17599	5	40	350
Flyback	2	Texas Instruments	LM5161PWPBKEVM	12	12	300

connected or disconnected according to the signal received from the microcontroller board, which is commanded by a personal computer. The voltage source consists of a 50 Hz ac signal that is rectified to a voltage level between 240 and 300 Vdc, as the high voltage bus of the aircrafts. The oscilloscope acquires the electrical signals of the converter depending on the configuration (scale, coupling, and trigger) settled by the computer for each experiment. The measured data is sent to the computer and stored. The data acquisition system was programmed using Python.

C. Data Acquisition in the Laboratory

The experimental data is measured and stored, as explained in the previous section. The used converter was the commercial isolated dc/dc converter DCM3714xD2K31E0yzz manufactured by Vicor, which is a well-known provider of aircraft power systems. Table I gives the main specifications of this power converter. The analyzed converter works in the DCM below 10% of the rated power.

On the other hand, eight different dc–dc power converters were used to model the corresponding CPLs. The information related to the used converters is given in Table II. It can be seen that four different types of power converters (flyback, buck, buck–boost, and forward) were used with the purpose of modeling the real behavior of the loads in the aircrafts.

The value of the resistors connected to the output was calculated based on the maximum power that can be delivered by the voltage source of each dc–dc converter.

Fig. 8 shows the experimental setup. It is evident the complexity of the system and the number of elements involved in order to generate an appropriate dataset for the training of the neural networks. Each component of the setup described in Fig. 7 can be found in Fig. 8.

The equipment used to acquire the experimental data included a dc power supply (BK Precision 9205; BK Precision Corporation, Yorba Linda, CA, USA), a 4 channel oscilloscope (Tektronix MDO3024 200 MHz 2.5 GS/s; Tektronix, Beaverton, OR, USA), two high-frequency current probes (Tektronix TCP0030A 0.001-20 A 120 MHz; Tektronix, Beaverton, OR, USA) and two high-frequency voltage probes (Tektronix THDP200; Tektronix, Beaverton, OR, USA).

A total of 1512 experiments were conducted, where 1000 of them were used to train the neural networks and the remaining 512 experiments to test their accuracy.

IV. RESULTS

This section presents the results of the proposed modeling algorithm when it is applied to the data collected from the step-down converter in the laboratory. The performance of the model is compared against that of five state-of-the-art modeling techniques. Two of them are feed-forward neural networks that are used in regression problems, such as the NARX and wavelet neural networks (WNNs). The first one is based on [22] and the hyper-parameters are tuned by means of a grid search, while for the WNN, the procedure used is the one presented in [33], where the signals are subjected to a wavelet decomposition and the most representative components are selected to train the network. On the other hand, two other approaches are the polytopic model [17] and the state space averaging model [18], which were explained in Section I. In case of polytopic modeling, the general model of the dc–dc converter is generated as a combination of multiple models, which are obtained based on the operating points of the dc–dc converter. In case of the state space average model, a simple buck converter was considered to obtain the modeling transfer function. The last technique is a 1-D CNN, which is often used to classify time–series, since this deep neural

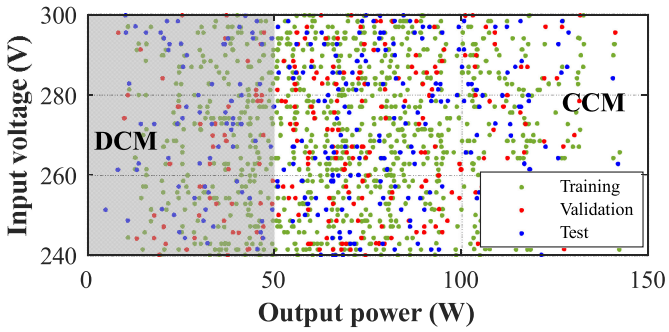

Fig. 9. Training, validation and test datasets plotted in the space defined by the output power and the input voltage of the converter.

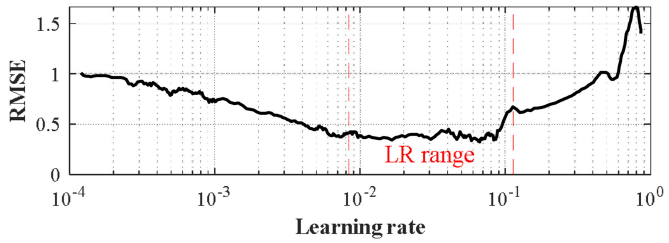

Fig. 10. LR test using the LSTM.

TABLE III
BAYESIAN OPTIMIZATION RANGE

Hyper-parameter	Minimum	Maximum	Optimal
Neurons	5	100	96
Learning rate	Given by the LR range test		0.01415
Gradient decay factor (GDF)	0.8	0.99	0.9799
L2 regularization	1e-10	1e-2	9.06e-7

network is able to identify complex signal patterns by applying filters. Datasets and codes are available upon request.

Fig. 9 shows the dataset dealt with, including the training, validation and test datasets, as a scatter graph where each point represents an experiment. The *x*-axis refers to the power delivered and the *y*-axis to the input voltage of the converter. The gray and white areas in Fig. 9 refer to the DCM and CCM of the dc–dc converter, respectively.

After obtaining the experimental results, the next step is to tune the hyper-parameters of the LSTM-NN. To determine the optimum LR range, the LR range test was applied, thus obtaining the RMSE for each LR value. Fig. 10 shows the RMSE evolution when it is tested under different LRs. The same phenomenon is seen in Fig. 5.

The next step is to apply the BOA to the measured data. The BOA was applied to 30 LSTM-NNs with different hyperparameter configurations, while each LSTM-NN was trained for 80 epochs. The algorithm was programmed in MATLAB using the Deep Learning Toolbox, and the training process was carried out using a GeForce RTX 2080 Super GPU. Table III gives the minimum, maximum and tuned values of the hyper-parameters used in the Bayesian optimization. The boundaries of the other hyperparameters are set based on their typical values and the complexity that a large value can add to the training process [27], [28].

TABLE IV
RMSE AND COEFFICIENT OF DETERMINATION (R^2)

Method	RMSE		R^2		Time elapsed
	I_{in}	V_{out}	I_{in}	V_{out}	
Proposed approach	0.0185	0.0172	0.991	0.985	1718.63 s
NARX-NN [22]	0.0401	0.0342	0.948	0.902	117915 s
Wavelet NN	0.0277	0.0241	0.966	0.930	842 s
Polytopic model [17]	0.0392	0.0366	0.910	0.844	427.0 s
State-space averaging method [18], [34]	0.0547	0.0360	0.849	0.774	233.2 s
1D CNN	0.0295	0.0212	0.960	0.948	2607.07 s

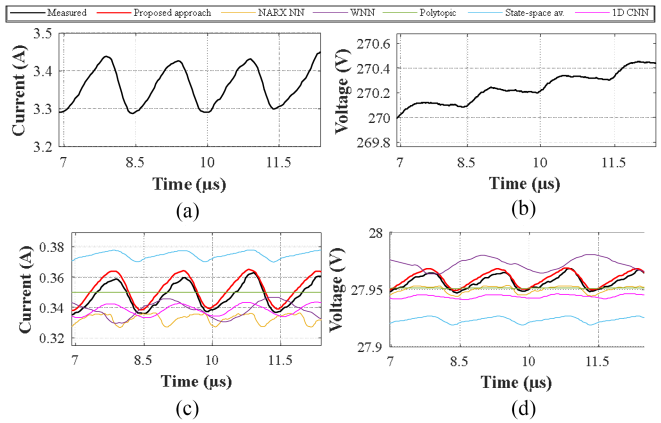

Fig. 11. Steady state comparison in CCM. (a) Output current. (b) Input voltage. (c) Input current. (d) Output voltage.

The next step is to train the LSTM-NN with the tuned hyperparameters, the number of epochs was set to 300 with a validation frequency of 15. Table IV gives the RMSE and coefficient of determination (R^2) mean values of the predictions of 512 different experiments from the test dataset. It shows the performance of the trained LSTM-NN and compares them to the results obtained with the other methods. The stopping criteria of the NARX-NN, polytopic model and the state-space averaging method are found in the references in Table IV. In case of the WNN and the 1-D CNN, a high epoch number is set, and the training process stops when the RMSE value increases for five consecutive epochs. Table IV proves that the deep learning approach proposed in this article is more accurate considering that the RMSE is lower and the R^2 is closer to 1, compared to the other analyzed modeling techniques. The polytopic and the state-space average models low precision might be because they do not perform well when the converter changes from one conduction mode to another. Even though that the proposed approach is not the fastest method, it takes a relatively short training time.

Figs. 11–14 compare the estimations of the proposed method with measurements and the state-of-the-art approaches. Each figure includes four plots. While (a) and (b) refer to the inputs applied to the model, (c) and (d) show the outputs (estimations). Figs. 11 and 12 present waveforms of the ripple during steady state in CCM ($V_{\text{in}} = 270$ V, $P = 94.5$ W), and in DCM ($V_{\text{in}} = 247$ V, $P = 22.3$ W), respectively.

The proposed approach is the only one able to replicate the waveforms in steady state (ripple, frequency, mean value) with

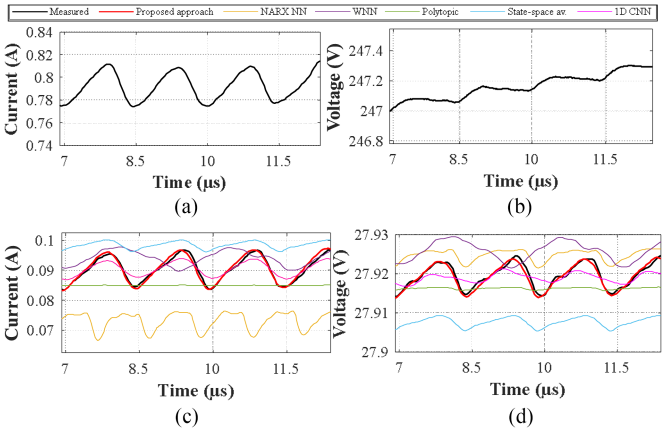

Fig. 12. Steady state comparison in DCM. (a) Output current. (b) Input voltage. (c) Input current. (d) Output voltage.

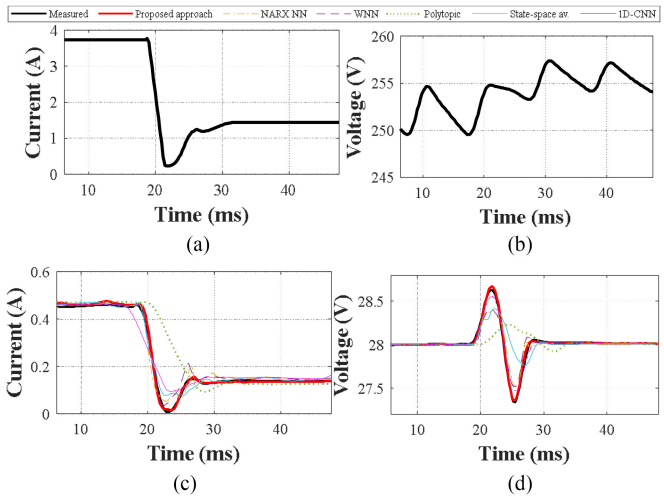

Fig. 13. Transient response during a load disconnection. (a) Output current. (b) Input voltage. (c) Input current. (d) Output voltage.

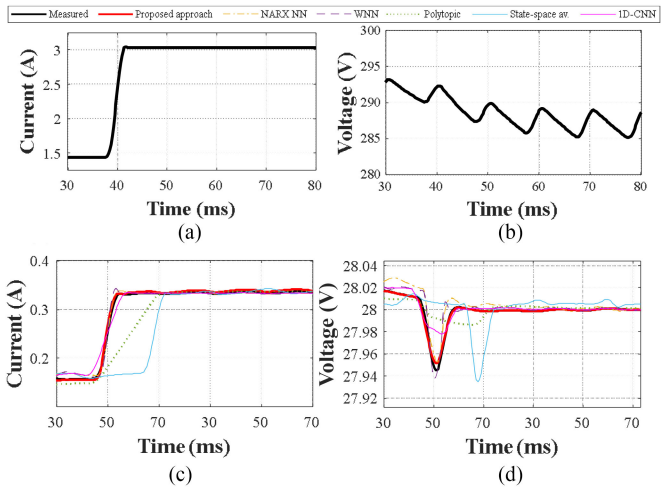

Fig. 14. Transient response during a load connection. (a) Output current. (b) Input voltage. (c) Input current. (d) Output voltage.

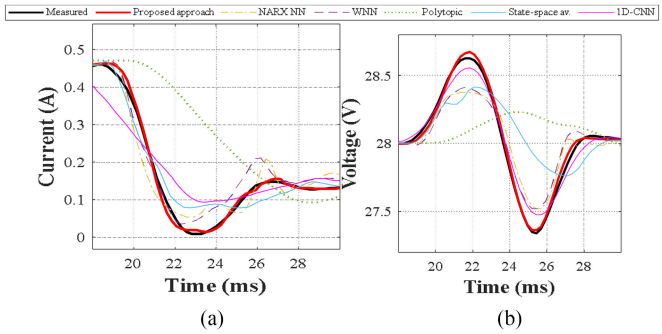

Fig. 15. Instantaneous response of the converter during a load disconnection. (a) Input current. (b) Output voltage.

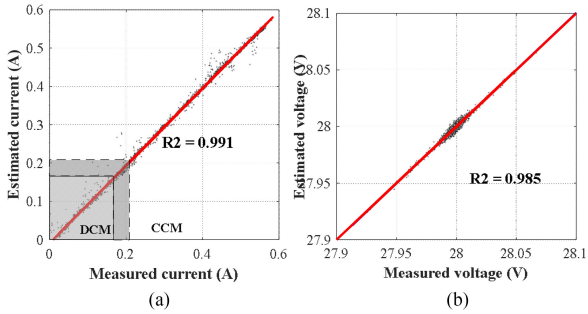

Fig. 16. Scatter plot of experimental versus estimations. (a) Input current. (b) Output voltage.

high fidelity in both CCM and DCM, the other methods present an inferior performance. The irregular distortion observed in the measured ripples of the signals is caused because measurements of dc–dc converters are often corrupted with high-frequency noise, which results from the switching characteristics of the converter and the sensor overamplification of the noise [35]. Figs. 13 and 14 present the transient response of the converter, the first one considers a load disconnection ($V_{\text{in}} = 252$ V, $P_{\text{initial}} = 116$ W, $P_{\text{final}} = 34.81$ W) and load connection ($V_{\text{in}} = 288$ V, $P_{\text{initial}} = 46.08$ W, and $P_{\text{final}} = 97.34$ W).

The estimated transient response for all models is similar. However, the LSTM-NN is the only one capable of replicating the overshoot of the signals. To better appreciate this effect, Fig. 15 shows a closer look to the first perturbation.

Results presented in Fig. 15 show that the proposed method replicates the instant transient response of the converter with high precision and outperforms the other approaches.

Finally, Fig. 16 shows a scatter plot comparing the measured and estimated currents in order to prove the robustness of the proposed method. The points of the graphs were calculated by using the test dataset (512 experiments) and the output values of the model obtained in the study. The plot in Fig. 16(a) is separated in three regions. The white region refers to the CCM of the converter, the light gray region to the DCM and the dark gray region is an area where the operating mode can be either CCM or DCM depending on the input voltage value. The graphs show a good generalization ability of the neural network since the dispersion between measured and estimated values is very low and the slope is almost 1 in both cases, which implies

a high correlation and accuracy. The few anomalies observed in the estimations of the current (i.e., $I_{\text{meas}} = 0.19$ A and $I_{\text{est}} = 0.276$ A) occur when the converter changes its operation from CCM to DCM and the model fails to replicate with high accuracy the overshoot of the instantaneous transient response. This phenomenon was only observed in 7 of the 102 cases (6.86%), and it does not affect the steady state estimation or the estimated response time.

V. Conclusion

This article has proposed an offline black-box modeling approach of a MEA 270 to 28 V step-down dc–dc converter used in aircrafts. To this end, a LSTM-NN was trained as it uses a BOA to tune a set of hyperparameters that enhances the accuracy of the model. The results presented in this article are based on an experimental setup, where multiple experiments considering different situations were carried out to train the neural networks. Such results show that the deep learning approaches have a higher accuracy when it is compared to existing methods in the literature. It was proven that the output prediction matches well with the actual output values given that the R^2 is 0.99, so that the neural network is able to predict the step-down converter steady-state and transient waveforms under CCM and DCM operating conditions. This identification method can be extended to other power electronics devices.

References

[1] Y. Zhang *et al.*, "Improved step load response of a dual-active-bridge DC–DC converter," *Electronics*, vol. 7, no. 9, pp. 185–200, Sep. 2018.

[2] Q. Wu, M. Wang, W. Zhou, X. Wang, and Q. Wang, "One zero-voltage-switching voltage-fed three-phase push-pull DC/DC converter for electric vehicle applications," in *Proc. IEEE Transp. Electrific. Conf. Expo*, 2019, pp. 1–5.

[3] V. Valdivia, A. Barrado, A. Lazaro, M. Sanz, D. Lopez Del Moral, and C. Raga, "Black-box behavioral modeling and identification of DC-DC converters with input current control for fuel cell power conditioning," *IEEE Trans. Ind. Electron.*, vol. 61, no. 4, pp. 1891–1903, Apr. 2014.

[4] Q. Shen, L. Ren, C. Gong, and H. Wang, "A unified feature parameter extraction strategy based on system identification for the buck converter with linear or nonlinear loads," in *Proc. 42nd Annu. Conf. IEEE Ind. Electron. Soc.*, 2016, pp. 388–393.

[5] A. Bréard, R. Moulla, and C. Vollaire, "Metamodel of power electronic converters using learning SVR method coupling with wavelet compression," *IEEE Trans. Electromagn. Compat.*, vol. 58, no. 2, pp. 588–598, Apr. 2016.

[6] L. Arnedo, R. Burgos, D. Boroyevich, and F. Wang, "System-Level black-box dc-to-dc converter models," in *Proc. IEEE Appl. Power Electron. Conf. Expo.*, 2009, pp. 1476–1481.

[7] H. Balakrishnan, M. Moreno-Ezuilaz, J.-R. Riba, S. Bogarra, and A. Garcia, "DC-DC buck converter parameter identification based on a white-box approach," in *Proc. IEEE 18th Int. Power Electron. Motion Control Conf.*, 2018, pp. 242–247.

[8] V. Valdivia, "Behavioral modeling and identification of power electronics converters and subsystems based on transient response," Universidad Carlos III de Madrid, Getafe, Spain, 2013.

[9] G. Rojas-Dueñas, J.-R. Riba, and M. Moreno-Eguilaz, "Non-Linear least squares optimization for parametric identification of DC-DC converters," *IEEE Trans. Power Electron.*, vol. 36, no. 1, pp. 654–661, Jun. 2021.

[10] O. Nelles, *Nonlinear System Identification. From Classical Approaches to Neural Networks and Fuzzy Models.* Berlin, Germany: Springer, 2001.

[11] L. Arnedo, R. Burgos, F. Wang, and D. Boroyevich, "Black-box terminal characterization modeling of DC-to-DC converters," in *Proc. IEEE Appl. Power Electron. Conf. Expo.*, 2007, pp. 457–463.

[12] A. Naziris, G. Guarderas, A. Frances, R. Asensi, and J. Uceda, "Large-signal black-box modelling of bidirectional battery charger for electric vehicles," in *Proc. IEEE Appl. Power Electron. Conf. Expo.*, 2019, pp. 3195–3198.

[13] S. K. Ki and R. Todd, "Black-box modelling of a permanent magnet generator for aerospace systems," in *Proc. Int. Conf. Electron., Mach. Drives.*, 2016, pp. 1–15.

[14] H. Ali, H. Liu, X. Zheng, P. Gao, and H. Zaman, "Frequency response based behavioral modeling verification for three phase AC-DC converter," in *Proc. 43rd Annu. Conf. IEEE Ind. Electron. Soc.*, 2017, pp. 4908–4912.

[15] M. Amara, C. Vollaire, M. Ali, and F. Costa, "Black box EMC modeling of a three phase inverter," in *Proc. Int. Symp. Electromagn. Compat.*, 2018, pp. 1–6.

[16] F. Alonge, R. Rabbeni, M. Pucci, and G. Vitale, "Identification and robust control of a quadratic DC/DC boost converter by hammerstein model," *IEEE Trans. Ind. Appl.*, vol. 51, no. 5, pp. 3975–3985, Sep. 2015.

[17] A. Frances, R. Asensi, and J. Uceda, "Blackbox polytopic model with dynamic weighting functions for DC-DC converters," *IEEE Access*, vol. 7, pp. 160263–160273, 2019.

[18] L. Wang *et al.*, "Electromagnetic transient modeling and simulation of power converters based on a piecewise generalized state space averaging method," *IEEE Access*, vol. 7, pp. 12241–12251, 2019.

[19] A. Nabinejad, A. Rajaei, and M. Mardaneh, "A systematic approach to extract state-space averaged equations and small-signal model of partial-power converters," *IEEE J. Emerg. Sel. Top. Power Electron.*, vol. 8, no. 3, pp. 2475–2483, Sep. 2020.

[20] P. Qashqai, K. Al-Haddad, and R. Zgheib, "Modeling power electronic converters using a method based on long-short term memory (LSTM) networks," in *Proc. Ind. Electron. Conf.*, 2020, pp. 4697–4702.

[21] T. Ergen and S. S. Kozat, "Online training of LSTM networks in distributed systems for variable length data sequences," *IEEE Trans. Neural Netw. Learn. Syst.*, vol. 29, no. 10, pp. 5159–5165, Oct. 2018.

[22] G. Rojas-Duenas, J.-R. Riba, K. Kahalerras, M. Moreno-Eguilaz, A. Kadechkar, and A. Gomez-Pau, "Black-Box modelling of a DC-DC buck converter based on a recurrent neural network," in *Proc. IEEE Int. Conf. Ind. Technol.*, 2020, pp. 456–461.

[23] S. Hochreiter and J. Schmidhuber, "Long short-term memory," *Neural Comput.,* vol. 9, no. 8, pp. 1735–1780, Nov. 1997.

[24] S. Wang, X. Wang, S. Wang, and D. Wang, "Bi-directional long short-term memory method based on attention mechanism and rolling update for short-term load forecasting," *Int. J. Elect. Power Energy Syst.*, vol. 109, pp. 470–479, Jul. 2019.

[25] I. Sutskever, O. Vinyals, and Q. V. Le, "Sequence to sequence learning with neural networks," 2014.

[26] S. Zhang, T. Liang, and V. Dinavahi, "Machine learning building blocks for real-time emulation of advanced transport power systems," *IEEE Open J. Power Electron.*, vol. 1, no. 1, pp. 488–498, Nov. 2020.

[27] A. H. Victoria and G. Maragatham, "Automatic tuning of hyperparameters using bayesian optimization," *Evol. Syst.*, vol. 12, pp. 217–223, May 2020.

[28] L. N. Smith, "A disciplined approach to neural network hyper-parameters: Part 1 – learning rate, batch size, momentum, and weight decay," Mar. 2018.

[29] B. Shahriari, K. Swersky, Z. Wang, R. P. Adams, and N. De Freitas, "Taking the human out of the loop: A review of Bayesian optimization," *Proc. IEEE*, vol. 104, no. 1, pp. 148–175, Jan. 2016.

[30] P. I. Frazier and J. Wang, "Bayesian optimization for materials design," *Inf. Sci. Mater. Discovery Des.*, vol. 225, pp. 45–75, 2015.

[31] S. Pang *et al.*, "Interconnection and damping assignment passivity-based control applied to on-board DC-DC power converter system supplying constant power load," *IEEE Trans. Ind. Appl.*, vol. 55, no. 6, pp. 6476–6485, Nov. 2019.

[32] M. Tariq, A. I. Maswood, C. J. Gajanayake, and A. K. Gupta, "Modeling and integration of a lithium-ion battery energy storage system with the more electric aircraft 270 v DC power distribution architecture," *IEEE Access*, vol. 6, pp. 41785–41802, 2018.

[33] B. Doucoure, K. Agbossou, and A. Cardenas, "Time series prediction using artificial wavelet neural network and multi-resolution analysis: Application to wind speed data," *Renew. Energy*, vol. 92, pp. 202–211, Jul. 2016.

[34] M. Baumann, C. Weissinger, and H. G. Herzog, "System identification and modeling of an automotive bidirectional DC/DC converter," in *Proc. IEEE Veh. Power Propulsion Conf.*, 2019.

[35] K. Lakomy *et al.*, "Active disturbance rejection control design with suppression of sensor noise effects in application to DC-DC buck power converter," *IEEE Trans. Ind. Electron.*, early access, Feb. 2, 2021, doi: 10.1109/TIE.2021.3055187.

Gabriel Rojas-Dueñas was born in Bogotá Colombia. He received the B.S. degree in electrical engineering from the Universidad de Los Andes, Bogotá, Colombia, in 2016, and the M.S. degree in energy engineering in 2018 from the Universitat Politècnica de Catalunya, Barcelona, Spain, where he is currently working toward the Ph.D. degree in electrical engineering.

His current research interests include power electronics, machine learning and modeling of electronic devices.

Jordi-Roger Riba (Member, IEEE) was born in Igualada, Spain, in 1966. He received the M.S. and Ph.D. degrees in physics from the Universitat de Barcelona, Barcelona, Spain, in 1990 and 2000, respectively.

In 1992, he was with the Universitat Politècnica de Catalunya, Barcelona, where he is currently a Full Professor. He is also with the Motion Control and Industrial Applications Group, Terrassa, Spain. His current research interests include high-voltage engineering, predictive maintenance methods, modeling and simulation of electromagnetic devices, and electrical machines.

Manuel Moreno-Eguilaz received the M.S. and Ph.D. degrees in industrial engineering from the Universitat Politècnica de Catalunya (UPC), Barcelona, Spain, in 1993 and 1997, respectively.

He is currently with the Motion Control and Industrial Applications Group, Terrassa, Spain, and is also an Associate Professor with the Department of Electronic Engineering, UPC. His current research interests include power electronics, fault tolerant converters, and hybrid electric vehicles.